

Base Pairing Configuration and Stability of an Oligonucleotide Duplex Containing a 5-Chlorouracil-Adenine Base Pair[†]

Jacob A. Theruvathu, Cherine H. Kim, Daniel K. Rogstad, Jonathan W. Neidigh, and Lawrence C. Sowers*

Department of Basic Sciences, School of Medicine, Loma Linda University, Loma Linda, California 92350

Received May 8, 2009; Revised Manuscript Received July 2, 2009

ABSTRACT: Inflammation-mediated reactive molecules can damage DNA by oxidation and chlorination. The biological consequences of this damage are as yet incompletely understood. In this paper, we have constructed oligonucleotides containing 5-chlorouracil (CIU), one of the known inflammation damage products. The thermodynamic stability, base pairing configuration, and duplex conformation of oligonucleotides containing CIU paired opposite adenine have been examined. NMR spectra reveal that the CIU-A base pair adopts a geometry similar to that of the T-A base pair, and the CIU-A base pair-containing duplex adopts a normal B-form conformation. The line width of the imino proton of the CIU residue is substantially greater than that of the corresponding T imino proton; however, this difference is not attributed to a reduced thermal or thermodynamic stability or to an increased level of proton exchange with solvent. While the NMR studies reveal an increased level of chemical exchange for the CIU imino proton of the CIU-A base pair, the CIU residue is not a target for removal by the *Escherichia coli* mispaired uracil glycosylase, which senses damage-related helix instability. The results of this study are consistent with previous reports indicating that the DNA of replicating cells can tolerate substantial substitution with CIU. The fraudulent, pseudo-Watson–Crick CIU-A base pair is sufficiently stable to avoid glycosylase removal and, therefore, might constitute a persistent form of cellular DNA damage.

Emerging studies indicate that the DNA of mammalian cells can be damaged by reactive molecules generated from activated neutrophils (1–5). The damaging agents include hydrogen peroxide and hypochlorous acid, resulting in both oxidized and chlorinated bases. Among these damage products is 5-chlorouracil (CIU),¹ which could arise by chlorination and deamination of cytosine residues in DNA and nucleotides or chlorination of uracil bases present in nucleotide precursor pools (6–10) as shown in Figure 1. Previous studies have demonstrated that significant levels of CIU can be incorporated into the DNA of replicating cells when 5-chloro-2'-deoxyuridine (CldU) is added as a nucleotide precursor (11–14).

The impact of the replacement of thymine with CIU in duplex DNA is not yet known. Although CldU is incorporated into the DNA of replicating cells, it does induce toxicity, senescence, and sister-chromatid exchanges (15–20). In this paper, we have constructed synthetic oligonucleotides containing CIU residues at a defined position in a self-complementary duplex paired opposite adenine. The synthetic oligonucleotides have been

characterized by mass spectrometry, thermal melting studies and NMR spectroscopy. In the duplex, the CIU residue pairs with adenine, forming two hydrogen bonds in a geometry approaching that of a normal thymine-adenine Watson–Crick base pair. We observe that the replacement of thymine with CIU paired opposite adenine has only a slight impact on oligonucleotide stability, although the line width of the CIU imino proton broadens much faster with increasing temperature than does the corresponding thymine imino proton. The potential for single-proton transfer from within the intact base pair is considered. The CIU-containing oligonucleotide was probed with the repair glycosylase MUG, which is known to exploit reduced duplex stability in its search for target bases. Whereas CIU mispaired with guanine is readily repaired, CIU paired opposite adenine within the same sequence context is not repaired. These data suggest that the replacement of thymine with CIU does not significantly perturb the structure or dynamics of a DNA duplex.

MATERIALS AND METHODS

Oligonucleotide Synthesis. Commercially available 2'-deoxyuridine was converted to CldU using the method of Kumar et al. (21). The corresponding phosphoramidite of CldU was prepared by standard methods, as previously described (22). All other phosphoramidites were obtained from Glen Research (Sterling, VA). Oligonucleotide synthesis was conducted with an Expedite synthesizer from Applied Biosystems (Foster City, CA). Oligonucleotides containing CldU were deprotected with concentrated aqueous ammonia at room temperature for 24 h.

The sequence of the 12-mer oligonucleotide examined here is shown in Figure 2. Oligonucleotides were purified by two rounds of HPLC, first with the DMT group on and the second with the

[†]This work is supported by grants from the National Institutes of Health.

*To whom correspondence should be addressed. Telephone: (909) 558-4480. Fax: (909) 558-4035. E-mail: lsowers@llu.edu.

Abbreviations: CIU, 5-chlorouracil; MUG, mispaired uracil DNA glycosylase; DMT, dimethoxytrityl; GC–MS, gas chromatography–mass spectrometry; MALDI-TOF-MS, matrix-assisted laser desorption ionization time-of-flight mass spectrometry; WATERGATE, water suppression through gradient tailored excitation; DSS, 4,4-dimethyl-4-silapentane-1-sulfonate; *T*_m, melting temperature; EDTA, ethylenediaminetetraacetic acid; NOE, nuclear Overhauser effect; DTT, dithiothreitol; DMSO, dimethyl sulfoxide; FU, 5-fluorouracil; BrU, 5-bromouracil; dUMP, 2'-deoxyuridine monophosphate; TMP, thymidine monophosphate.

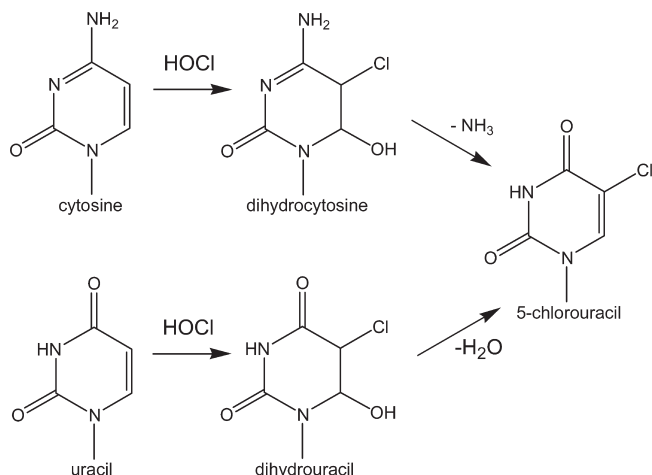


FIGURE 1: Formation of 5-chlorouracil (CIU). CIU can be generated by two routes. Initial reaction of cytosine with HOCl can result in formation of the dihydro intermediate, which can then deaminate and dehydrate, generating CIU (top pathway). Alternatively, uracil can react with HOCl forming a dihydro intermediate and then dehydrate forming CIU (bottom pathway).

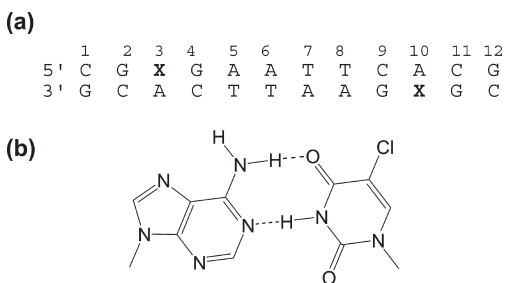


FIGURE 2: Oligonucleotide sequences. (a) 12-mer oligonucleotide sequence used for the study (X = 5-chlorouracil). (b) Watson-Crick base pairing of a CIU-A base pair.

DMT group off. Oligonucleotides were examined by MALDI-TOF-MS (23), and the free base composition was verified by GC-MS following acid hydrolysis (24).

Oligonucleotide UV Melting Studies. The melting temperature (T_m) and thermodynamic values of the oligonucleotide were obtained as previously described (23, 30) using a Varian (Palo Alto, CA) Bio 300 Cary UV-vis spectrophotometer. The self-complementary oligonucleotide at various concentrations (2–60 μ M) was dissolved in a buffer containing 100 mM NaCl, 0.1 mM EDTA, and 10 mM sodium phosphate (pH 7). The sample was then treated with a thermal cycle from 10 to 90 °C at an interval of 0.5 °C. The thermodynamic values were obtained from the average of five such temperature cycles. T_m values are reported at a total strand concentration of 28 μ M.

Nuclear Magnetic Resonance Spectroscopy (NMR). NMR spectra were obtained with a 500 MHz Bruker (Billerica, MA) NMR system. The proton NMR spectra of the oligonucleotide were recorded in a solution containing 10% D₂O, 100 mM NaCl, 10 mM sodium phosphate, and 0.2 mM EDTA (pH 7.0) and compared with results from similar sequences published by other laboratories (25–28). The oligonucleotide (200 A_{260} OD units, 2.5 mM) was annealed at 86 °C for 2 min and slowly cooled prior to acquisition of NMR spectra. Each spectrum was calibrated using DSS (4,4-dimethyl-4-silapentane-1-sulfonate) as an internal standard reference. Proton NMR spectra of oligonucleotides in 90% H₂O were recorded with a water suppression double gradient echo WATERGATE

W5 pulse program (29). The temperature of the sample was controlled by a variable-temperature monitor (Eurotherm, BVT 3000) from Bruker.

A typical spectrum was acquired with a binomial water suppression delay (d19) of 160 μ s. Since the delay (d19) of 160 μ s affected some of the imino resonances near 11 ppm, it was changed to 40 μ s when high peaks for the imino protons were desired. The null point repetition was every 6.25 ppm from the suppression point when the d19 was 160 μ s. When the delay was 40 μ s, the null point repetition was far from any of the imino proton resonances. The line width studies were performed using the d19 delay of 40 μ s. The two-dimensional (2D) NOE spectra were acquired using a mixing time of 300 ms.

Mispaired Uracil Glycosylase (MUG) Reaction with CIU Oligo. The glycosylase studies were performed using mispaired uracil glycosylase (MUG) from *Escherichia coli* (30). A typical reaction was conducted by reacting 300 pmol of oligonucleotide with 14.7 pmol of enzyme in a buffer containing 20 mM NaCl, 20 mM Tris-HCl, 1 mM EDTA, and 1 mM DTT (pH 8). The reaction mixture was incubated at 37 °C overnight. The sample was then desalted for MALDI-TOF analysis with a P6 column and a cation exchange column containing AG50W-X8 beads on the H⁺ form (Bio-Rad, Hercules, CA). MALDI-TOF experiments were performed with a Bruker Autoflex time-of-flight mass spectrometer operated in positive ion and reflectron modes (23).

RESULTS

Oligonucleotides containing CIU at a defined site were prepared by standard phosphoramidite methods. Commercially available dU was converted to CldU using a previously reported method (18). Oligonucleotides containing CIU were synthesized, deprotected, and purified using standard conditions (Figure 2), except that deprotection was conducted in concentrated aqueous ammonia at room temperature for 24 h. The base composition of each oligonucleotide was verified by GC-MS following acid hydrolysis (Figure 3). Because of the high natural abundance of both ³⁵Cl and ³⁷Cl isotopes, the mass spectrum of chlorine-containing molecules has a significant M + 2 line for the parent ion and M – methyl ion. Intact oligonucleotides were also examined by MALDI-TOF-MS as shown in Figure 3. The isotope envelope of larger molecules can also be simulated, and the presence of one chlorine atom in the oligonucleotide profoundly impacts the shape of the isotope envelope. The simulated ion cluster of an oligonucleotide of composition C₁₁₆H₁₄₅N₄₅O₇₀P₁₁Cl is shown above and matches the experimental spectrum in Figure 3a. The theoretical and observed masses for each of the oligonucleotides examined here are as follows: 3644.65 and 3644.61 for T-A, 3664.59 and 3664.54 for CIU-A, and 3680.59 and 3680.54 for CIU-G, respectively.

The thermal stability of the oligonucleotide duplex (31–33) containing CIU was examined and compared with that of an oligonucleotide containing T. The melting temperature of the CIU-containing oligonucleotide was observed to be 55.6 °C, while that of the control oligonucleotide containing T was 53.4 °C. Thermodynamic parameters obtained are listed in Table 1. The thermal melting profiles of the T and CIU-containing oligonucleotides are shown in Figure 4.

Proton NMR spectra of the monomers of thymidine and CldU were recorded as references for oligonucleotide-induced changes in chemical shifts. The H6 proton resonances of dT and CldU in

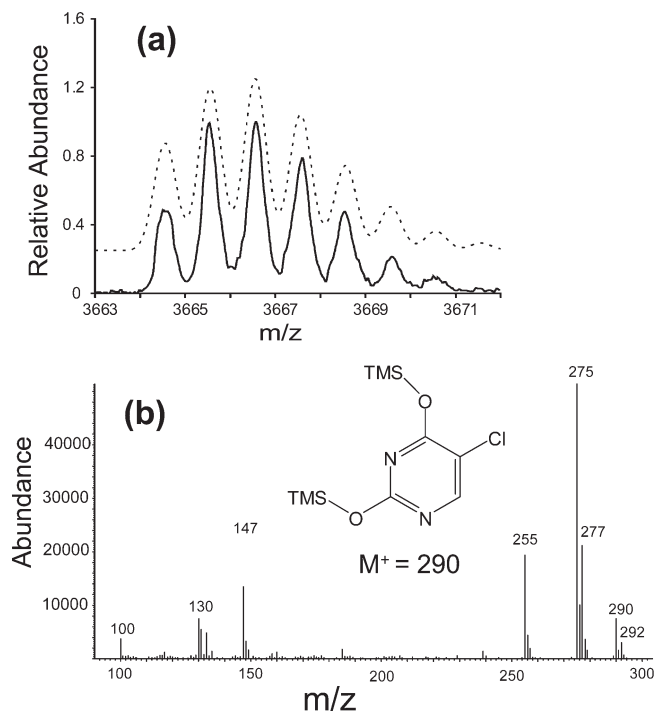


FIGURE 3: Oligonucleotide analysis by mass spectrometry. (a) Experimental (bottom) and theoretical (top) isotope envelope of the 12-mer oligonucleotide 5'-CGCIUGAATTCACG-3' used in this study. The experimental isotope envelope was obtained from MALDI-TOF mass spectrometry, and the theoretical envelope was obtained using a computer simulation program (23). (b) GC-MS spectrum of CIU after acid hydrolysis of CIU-A oligonucleotide. Molecules containing chlorine are easily recognized by the prominent $M + 2$ peaks (277 and 292 amu) in the mass spectrum.

Table 1: Thermal Melting and Thermodynamic Parameters for the Helix-Coil Transition of 5'-d(CGXGAATTCACG)-3' in 10 mM Sodium Phosphate, 100 mM Sodium Chloride, and 0.1 mM EDTA (pH 7.0)

	T-A	CIU-A
T_m (°C)	53.4 ± 0.3	55.6 ± 0.3
ΔH° (kcal/mol)	-85 ± 13	-81 ± 14
ΔS° (cal mol $^{-1}$ K $^{-1}$)	-238 ± 40	-234 ± 4
ΔG° (kcal/mol)	-11.9 ± 1.0	-12.2 ± 1.0
hyperchromicity (%)	22.0 ± 0.6	21.3 ± 0.8

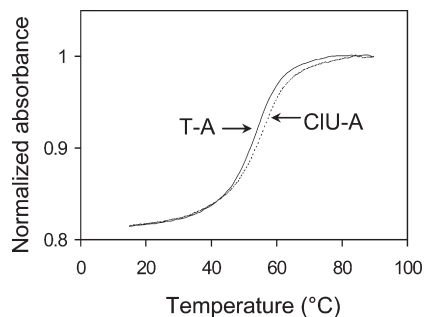


FIGURE 4: Oligonucleotide melting profiles examined by temperature-dependent absorbance at 260 nm: UV melting profiles (normalized) of 12-mer oligonucleotide 5'-CGXGAATTCACG-3' at 28 μ M in a buffer containing 100 mM sodium chloride, 10 mM sodium phosphate, and 0.1 mM EDTA (pH 7.0): T-A (—) and CIU-A (···).

D₂O were observed to be 7.64 and 8.17 ppm, respectively. The chemical shifts of the N3 imino proton resonances of dT and

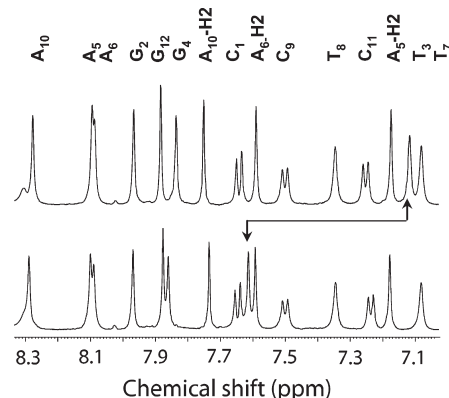


FIGURE 5: NMR spectrum of nonexchangeable protons. ^1H NMR spectra of the CIU-A (bottom) and T-A (top) oligonucleotides in the aromatic region. The H6/H8 and H2 assignments are written atop the spectrum. H6 of CIU3 and T3 is indicated by the arrow. The spectra were recorded at 30 °C with 256 scans using a water suppression WATERGATE program with a binomial water suppression delay (d19) of 160 μ s. The oligonucleotide was dissolved in a buffer containing 10% D₂O, 100 mM sodium chloride, 10 mM sodium phosphate, and 0.2 mM EDTA (pH 7).

Table 2: Chemical Shifts of Aromatic Protons of the Oligonucleotide 5'-d(CGXGAATTCACG)-3' at pH 7.0 and 30 °C

nucleobase	H6/H8		H2/H5	
	T-A	CIU-A	T-A	CIU-A
C1	7.64	7.65	5.91	5.92
G2	7.97	7.97		
T3/CIU3	7.12	7.61		
G4	7.84	7.86		
A5	8.09	8.10	7.17	7.18
A6	8.09	8.09	7.59	7.59
T7	7.08	7.08		
T8	7.35	7.35		
C9	7.50	7.50	5.68	5.81
A10	8.28	8.29	7.75	7.73
C11	7.25	7.24	5.35	5.34
G12	7.88	7.88		

CldU in DMSO were observed to be 11.26 and 11.82 ppm, respectively. The imino proton of CIU is substantially more acidic than the corresponding imino proton of T. The pK of the CldU imino proton was measured by titration of the chemical shift of the H6 resonances and found to be 8.0 (Supporting Information).

Proton NMR spectra of the nonexchangeable protons of each duplex were obtained and are shown in Figure 5. Proton resonances were assigned by standard 2D methods (34) and are listed in Table 2. The corresponding 2D spectra are shown as Supporting Information. The observed proton connectivities indicate that both the T-A and CIU-A duplexes are predominantly in a B-form geometry and all bases are intrahelical. The H6 proton for T3 of the T-A oligonucleotide is observed at 7.12 ppm, whereas the corresponding H6 proton of the CIU residue of the CIU-A duplex was observed at 7.61 ppm.

Proton spectra of the exchangeable proton resonances were recorded in 90% H₂O and 10% D₂O, and the spectra of the T-A and CIU-A duplexes are shown in Figure 6. Proton resonances were assigned by standard 2D methods, as described previously. The assignments are recorded in Table 3. The N3 imino proton of T in position 3 of the oligonucleotide was observed at 13.71 ppm

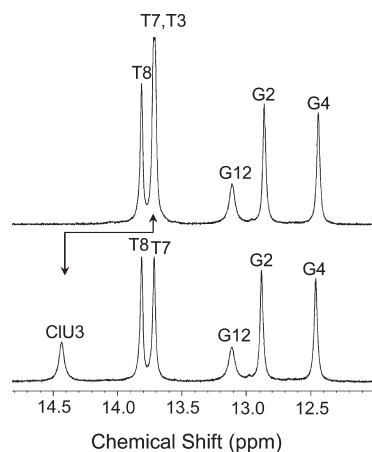


FIGURE 6: NMR spectrum of exchangeable protons. ^1H NMR spectrum of the CIU-A (bottom) and T-A (top) oligonucleotides in the imino region. The spectra were recorded at 5°C with 256 scans using a water suppression WATERGATE program with a binomial water suppression delay (d19) of $40\ \mu\text{s}$. The oligonucleotide was dissolved in a buffer containing 10% D_2O , 100 mM sodium chloride, 10 mM sodium phosphate, and 0.2 mM EDTA (pH 7).

Table 3: Chemical Shifts of Imino Protons of the Oligonucleotide 5'-d(CGXGAATTCACG)-3' at pH 7.0 and 5°C

nucleobase	imino protons	
	T-A oligo	CIU-A oligo
G2	12.86	12.88
T3/CIU3	13.71	14.43
G4	12.44	12.46
T7	13.72	13.72
T8	13.81	13.81
G12	13.11	13.11

and for CIU 14.43 ppm. The line width of the proton resonance assigned to the CIU imino proton was greater than most others in the duplex and significantly more broad than the width of the imino resonance of the corresponding T-A proton. The width of this proton increased rapidly with an increase in temperature (Figure 7). The rapid line broadening of the CIU imino proton appeared to be independent of solution pH (Figure 7c).

The imino proton region of the CIU-A base pair examined here is shown in Figure 8. The imino proton region of the duplex at 5°C and pH 7.0 is shown in Figure 8a. Under these conditions, the CIU and terminal G imino proton resonances are significantly broader than the remaining imino proton resonances. With an increase in the solution pH to 8.8, the imino proton of the terminal G-C base pair broadens further and is lost from the spectrum, whereas the CIU imino proton has neither broadened nor shifted (Figure 8b). An increase in sample temperature from 5 to 22°C at pH 7.0 results in broadening and loss of both the terminal G-C and CIU imino protons (Figure 8c).

The enzymatic repair of CIU was investigated by probing the CIU-containing oligonucleotide with the repair glycosylase, MUG. A positive control sequence in which the CIU was paired opposite guanine was probed with MUG, and the CIU was rapidly removed (Figure 9). Enzymatic removal of the CIU residue generates an oligonucleotide containing an abasic site. The theoretical mass of the abasic site-containing oligonucleotide is 3552.59 amu, and the observed mass is 3552.50 amu. The observed reduction in the oligonucleotide mass by 128 amu

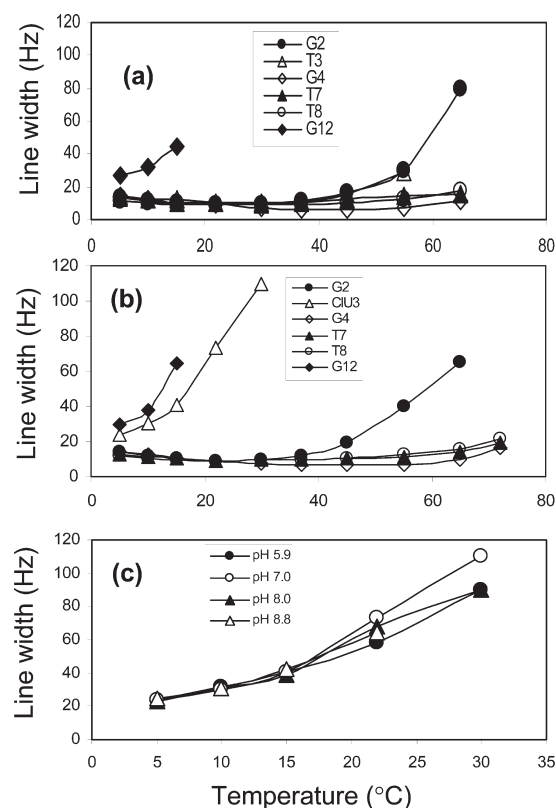


FIGURE 7: Line widths of imino protons as a function of temperature and pH. (a) Temperature-dependent imino proton line widths of different base pairs of T-A oligonucleotide at pH 7.0. (b) Temperature-dependent imino proton line widths of different base pairs of CIU-A oligo at pH 7.0. (c) Temperature-dependent imino proton line widths of the CIU-A (3) base pair of CIU-A oligo at pH, 5.9, 7.0, 8.0, and 8.8. The oligonucleotide was dissolved in a buffer containing 10% D_2O , 100 mM sodium chloride, 10 mM sodium phosphate, and 0.2 mM EDTA.

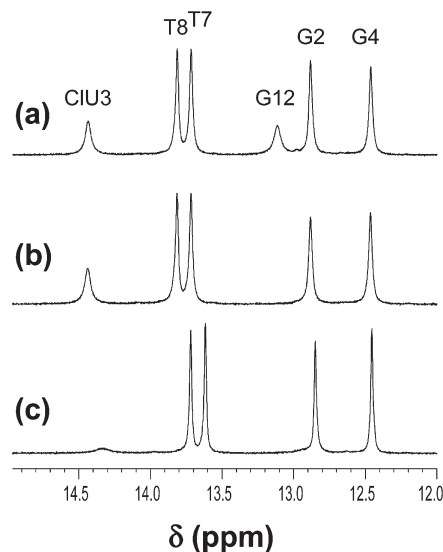


FIGURE 8: ^1H NMR spectrum of the CIU-A oligonucleotide in the imino region at different pH and temperatures: (a) pH 7.0 and 5°C , (b) pH 8.8 and 5°C , and (c) pH 7.0 and 22°C . The spectra were recorded with 256 scans using a water suppression WATERGATE program with a binomial water suppression delay (d19) of $40\ \mu\text{s}$. The oligonucleotide was dissolved in a buffer containing 10% D_2O , 100 mM NaCl, 10 mM sodium phosphate, and 0.2 mM EDTA.

results from the displacement of CIU ($-145\ \text{amu}$) by a hydroxyl group ($17\ \text{amu}$). Under identical reaction conditions, neither

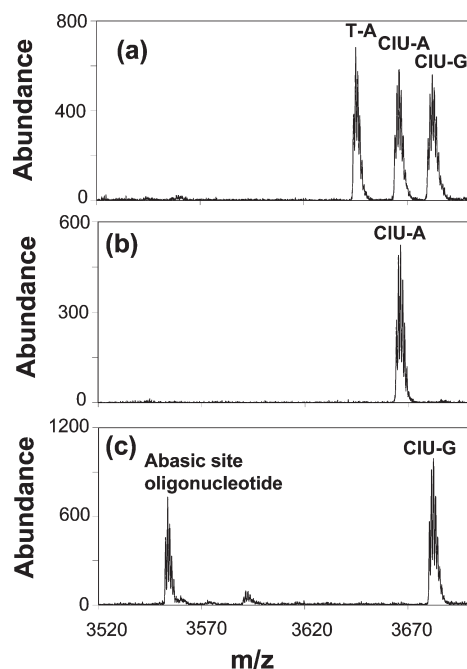


FIGURE 9: Activity of MUG on synthetic oligonucleotides containing CIU-A or CIU-G. MALDI spectra of oligonucleotides. (a) Mixture of T-A, CIU-A, and CIU-G oligonucleotides without enzymatic reaction. (b) CIU-A oligo reacted with MUG. (c) CIU-G oligonucleotide incubated with MUG. The enzyme reaction was conducted by reaction of 300 pmol of oligonucleotide with 14.7 pmol of enzyme in a buffer containing 20 mM sodium chloride, 20 mM Tris-HCl, 1 mM EDTA, and 1 mM DTT (pH 8). The incubation was at 37 °C for 20 h.

CIU (Figure 9) nor thymine (data not shown) paired opposite adenine is repaired.

DISCUSSION

Emerging studies show that DNA can be damaged by reactive molecules derived from activated neutrophils and eosinophils at sites of inflammation (1–9). Among the damage products are oxidized and halogenated pyrimidines, including CIU (Figure 1). It has been suggested that these damage products might provide a mechanistic link between inflammation and human diseases, including cancer (5).

It is well established that halogenated pyrimidines can be incorporated into nucleotide precursor pools and ultimately into DNA. FU (5-fluorouracil) is used as a chemotherapy agent as its metabolite (5'-fluoro-2'-deoxyuridine 5'-monophosphate) inhibits thymidylate synthase needed for the conversion of dUMP to TMP (35, 36). Some FU is also incorporated into DNA where it can be removed by several glycosylases (37, 38). BrU is a mutagenic base analogue long known to induce transition mutations, presumably by miscoding more frequently than T (39, 40). Replicating cells can tolerate substantial replacement of T with BrU (41, 42). Similarly, CIU can be incorporated into the DNA of replicating cells (6, 10–15). However, CIU has been shown to induce cellular toxicity, cause senescence, and increase the frequency of sister-chromatid exchanges (15–19). It has been proposed that the toxicity might in part be attributed to interference with nucleotide metabolism, which promotes dUTP misincorporation and repair by a mechanism similar to that proposed for FU (18). However, the mechanism of sister-chromatid exchange remains to be resolved.

Because of the recent interest in CIU in DNA, we have incorporated CIU into synthetic oligonucleotides to ascertain the base pairing configuration when paired opposite adenine and to examine the impact of CIU substitution on the stability of an oligonucleotide duplex. Oligonucleotides containing CIU were prepared and purified by standard methods (Figure 2). The phosphoramidite of CIU is prepared by standard methods, and no special deprotection conditions are required. The composition of oligonucleotides containing CIU can be verified by acid hydrolysis followed by GC–MS analysis (Figure 3). The presence of chlorine in a molecule profoundly impacts the corresponding mass spectra, allowing unambiguous identification of the chlorinated pyrimidine. Similarly, the presence of chlorine alters the MALDI-TOF-MS spectrum of the intact oligonucleotide (Figure 3).

To investigate the impact of the CIU substitution on oligonucleotide stability, oligonucleotide melting temperatures were determined by measuring UV absorbance as a function of temperature. Example results for the T-A and CIU-A duplexes are shown in Figure 4. In the CIU-A duplex, two CIU-A pairs are substituted for two T-A base pairs. The results show that substitution of T with CIU increases the oligonucleotide melting temperature by 2.2 °C. We note that the self-complementary sequence used here has two substitutions per duplex. Therefore, the change in melting temperature is approximately 1.1 °C per CIU substitution. Thermodynamic parameters were obtained by measuring T_m values as a function of oligonucleotide concentration. The values obtained are recorded in Table 1. The substitution of T with CIU, therefore, increases slightly the thermal and thermodynamic stability of an oligonucleotide duplex.

The duplex conformation and base pairing configuration were examined with NMR spectroscopic methods. All of the expected nonexchangeable proton resonances were observed for the T-A and CIU-A duplexes, as shown in Figure 5. The only difference between the two duplexes is that the protons of T_3 , and in particular the T_3 H6 proton resonance at 7.12 ppm, are lost upon substitution of T with CIU, with a corresponding gain of a proton resonance at 7.61 ppm assigned to the H6 proton of the CIU residue. The difference in the chemical shifts of the H6 protons of T and CIU is attributed to the difference in the electronic-inductive property of the 5-methyl versus 5-chloro substituent. The chemical shift of T_3 H6 moves upfield, relative to the monomer chemical shift, by 0.52 ppm, whereas that of H6 of CIU moves upfield by 0.56 ppm. The similar magnitude of the stacking-induced upfield shift indicates both the T and CIU experience similar base stacking and geometry relative to the bases above and below the helix. However, the greater relative stacking-induced shift of the CIU H6 proton is consistent with the observed increase in the thermodynamic stability of the CIU-containing duplex discussed above. The observed chemical shift of the H6 proton of CIU when paired with A indicates it is in the neutral and keto tautomeric form (28). The base-sugar connectivities observed indicate that the CIU-A duplex, as with the T-A duplex, is predominantly B-form.

The impact of the CIU substitution on base pair formation was investigated by examining exchangeable proton resonances. Exchangeable spectra are shown in Figure 6. The T_3 imino proton of the T-A duplex at 13.71 ppm is lost upon substitution with CIU; however, a new resonance is observed at 14.43 ppm, assigned to the CIU imino proton. The downfield shift in the N3 resonance from dT to CIdU of 0.72 ppm can be attributed

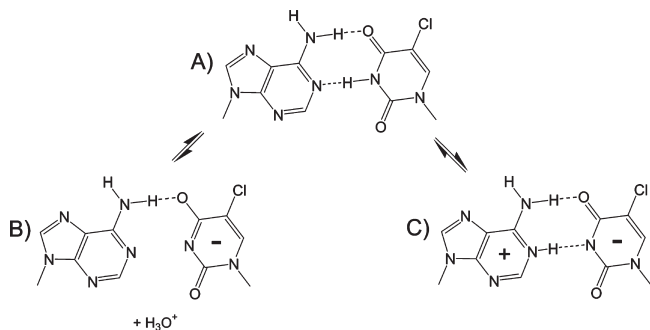


FIGURE 10: Proposed proton tunneling between CIU and A residues in a DNA duplex. (A) Neutral base pair in pseudo Watson–Crick geometry. (B) Ionized base pair resulting from exchange of the CIU N3 proton with solvent. (C) Base pair following transfer of a proton from CIU to A.

primarily to the opposing electronic inductive properties of the methyl and chloro substituents. The N3 resonances of dT and CldU monomers in DMSO are 11.26 and 11.82 ppm, respectively, a difference of 0.56 ppm. The observed chemical shift for an imino proton in an oligonucleotide is a function of both the intrinsic chemical shift and hydrogen bond formation. Upon substitution of T with CIU, the observed imino proton chemical shift moves further downfield than can be attributed exclusively to the intrinsic chemical shift difference. The observed data would suggest that the hydrogen bond formed by the N3 proton of CIU is stronger than that of the corresponding T base pair. The increased strength of this hydrogen bond is consistent with the increase in the observed acidity of the CldU imino proton as well as with results of theoretical studies (43). Consistent with the results reported here for the CIU–A base pair, previous NMR studies with both the FU–A (44, 45) and BrU–A (46) base pairs indicate base pair configurations similar to that of the T–A base pair.

The structural and thermodynamic properties of the T–A and CIU–A duplexes appear to be very similar in many ways. However, a distinguishing feature of the CIU–A pair is that the proton resonance assigned to the CIU imino proton is substantially broader than the corresponding T–A proton within the same sequence context (Figures 7 and 8): the line width of the T imino proton of the T–A duplex at 30 °C is 10.7 Hz, whereas the line width of the corresponding CIU imino proton of the CIU–A duplex is 110 Hz. We considered the possibility that base-catalyzed exchange of the more acidic CIU imino proton might destabilize and reduce the lifetime of the CIU–A base pair as shown in Figure 10B. Increasing the solvent pH from 7.0 to 8.8 at 5 °C results in broadening of the terminal G:C imino protons, which can be attributed to an increased rate of base pair opening (47, 48). However, the CIU–A imino proton is neither shifted nor broadened, although the solution pH has been increased to nearly 1 pH unit above the pK_a of the monomer, CldU. This result indicates that formation of the CIU–A base pair sequesters the imino proton, suppressing the transfer of the CIU imino proton to solvent water. Indeed, the results of theoretical calculations (43) suggest that the CIU–A imino proton hydrogen bond is both shorter and stronger than the corresponding bond in the T–A base pair, consistent with the hydrogen bonding-induced shifts as discussed above.

The observed broadening of the CIU–A base pair cannot be attributed to reduced duplex stability as the oligonucleotide containing the CIU–A base pair is more thermally and thermodynamically stable than the corresponding T–A control

oligonucleotide (Figure 4 and Table 1). Previously, Sternglanz and Bugg concluded from examination of the crystal structures of 5-chloro- and 5-bromouracil that halogenated uracil analogues may have enhanced base stacking interactions (49). The line widths of the imino protons of the base pairs above and below the CIU–A base pair are identical with the line widths of the corresponding protons observed for the T–A oligonucleotide control, indicating that the CIU–A base pair does not create a denaturation bubble within the helix. The observed broadening of the CIU–A imino proton cannot be attributed to enhanced exchange with solvent as discussed above. We therefore considered the possibility that the broadening of the CIU–A imino proton might result from proton exchange from within the intact base pair.

Previously, Shulman (50) considered single-proton transfer of the N3 imino proton of T to the complementary A residue in a Watson–Crick T–A base pair. Single-proton transfer renders the T residue anionic and the A residue protonated. The energy cost for this transfer is the sum of the energetic cost of ionizing both the T and A monomers at pH 7.2 and is estimated to be approximately 7.6 kcal/mol so that the zwitterionic base pair would be present at a frequency of approximately one in 3.8×10^5 A–T base pairs. Replacement of the electron-donating 5-methyl group of T with the electron-withdrawing chloro substituent of CIU reduces the pK_a of the N3 imino proton from 9.8 to 7.9–8.0. The energy cost of ionizing the CIU therefore drops the free energy of proton transfer by 2.6 kcal/mol to approximately 5.0 kcal/mol (51), increasing the frequency of the zwitterionic base pair shown in Figure 10C by a factor of approximately 80, relative to the canonical T–A base pair. Previous studies have demonstrated that base damage and ion binding can also facilitate inter-base pair single-proton transfer (52, 53).

The pK_a of the N3 position of monomeric 2′-deoxyadenosine is approximately 3.8 in solution (28). However, in some base pairing configurations, the pK_a of the N3 position of an adenine residue has been observed to increase to > 7.0 (54–56). Recent studies suggest that adenine protonation in a duplex can further stabilize base stacking interactions and can facilitate the formation of some nucleic acid structural motifs. Possibly, thermal motions that disrupt normal base stacking interactions could be offset by single-proton transfer and adenine protonation. The reduced energy of single-proton transfer for the CIU–A base pair might partially account for the slight increase in the stability of the CIU–A-containing duplex.

The results of the physical studies described above suggest that the CIU substitution does not significantly alter the overall duplex structure or base pairing configuration and increases slightly duplex stability. The increased level of broadening of the CIU imino proton suggests possible increased base pair mobility. We therefore sought to determine if these modest structural fluctuations could be detected by DNA repair glycosylases. Previous studies from this lab and others (30, 37, 38) have demonstrated that repair glycosylases can find and distinguish damaged and modified bases in DNA upon the basis of reduced stability and changes in glycosidic bond strength. The electron-withdrawing 5-chloro substituent of CIU enhances glycosylase removal by several glycosylases relative to T, which has an electron-donating methyl substituent. Target bases mispaired with G are more easily repaired than those paired with A due to the reduced stability of the mispair. We probed the CIU-containing duplex examined here with the *E. coli* mispaired uracil DNA

glycosylase, MUG. We observed that CIU mispaired with G is readily removed by MUG, as shown in Figure 9. In contrast, CIU paired with A is not repaired. The apparent increased mobility of CIU when paired with A is insufficient to render the CIU base susceptible to glycosylase removal.

The similarity of the structures and stabilities of the oligonucleotides containing T-A and CIU-A base pairs demonstrated here is consistent with the results of studies showing that substantial amounts of CldU can be incorporated into the DNA of replicating cells (11–14). Substitution with CIU is not overtly toxic but is more subtle in causing chromosomal aberrations (15–20). The results of this study suggest that once incorporated, CIU can form a fraudulent base pair with adenine, undetected by DNA repair glycosylases. The adverse effects of CIU substitution might reveal themselves only in biologically important unusual DNA structures required for DNA replication, repair, or transcription. It is known that the thymine methyl group is important for the binding of sequence-specific DNA-binding proteins (57). While 5-bromo can substitute for 5-methyl in many DNA–protein interactions (58–60), 5-chloro is smaller and might perturb some DNA–protein interactions (61). On the other hand, one recent study suggests that 5-halogenated uracil residues in DNA could direct the formation of an unusual macromolecular conformation (62).

CONCLUSIONS

In this paper, we have investigated the base pairing configuration, duplex conformation, and thermodynamic stability of a model oligonucleotide duplex containing CIU. The CIU-A duplex is equivalent to the corresponding T-A duplex with respect to overall conformation and base pairing. The CIU-A base pair is slightly more stable than the T-A base pair and appears to adopt a similar geometry. Single-proton transfer would be more likely in the CIU-A base pair than in the T-A base pair, and the increased level of proton transfer from CIU to A could account in part for the apparent increased stability of the CIU-A-containing oligonucleotides. The CIU base, when paired with A, is sufficiently stable to escape detection and removal by repair glycosylases. The adverse biological effects of CIU could result from the disruption by CIU of biologically important unusual DNA structures or sequence-specific DNA protein interactions. Studies are currently in progress to investigate these possibilities.

SUPPORTING INFORMATION AVAILABLE

Additional experimental data and figures. This material is available free of charge via the Internet at <http://pubs.acs.org>.

REFERENCES

- Henderson, J. P., Byun, J., Takeshita, J., and Heineke, J. W. (2003) Phagocytes produce 5-chlorouracil and 5-bromouracil, two mutagenic products of myeloperoxidase, in human inflammatory tissue. *J. Biol. Chem.* 278, 23522–23528.
- Jiang, Q., Blount, B. C., and Ames, B. N. (2003) 5-Chlorouracil, a marker of DNA damage from hypochlorous acid during inflammation: A gas chromatography-mass spectrometry assay. *J. Biol. Chem.* 278, 32834–32840.
- Takeshita, J., Byun, J., Nhan, T. Q., Pritchard, D. K., Pennathur, S., Schwartz, S. M., Chait, A., and Heineke, J. W. (2006) Myeloperoxidase generates 5-chlorouracil in human atherosclerotic tissue: A potential pathway for somatic mutagenesis by macrophages. *J. Biol. Chem.* 281, 3096–3104.
- Knaapen, A. M., Gungör, N., Schins, R. P., Borm, P. J., and Van Schooten, F. J. (2006) Neutrophils and respiratory tract DNA damage and mutagenesis: A review. *Mutagenesis* 21, 225–236.
- Valinluck, V., and Sowers, L. C. (2007) Inflammation-mediated cytosine damage: A mechanistic link between inflammation and the epigenetic alterations in human cancers. *Cancer Res.* 67, 5583–5586.
- Hale, J. T., Bigelow, J. C., Mathews, L. A., and McCormack, J. J. (2002) Analytical and pharmacokinetic studies with 5-chloro-2'-deoxycytidine. *Biochem. Pharmacol.* 64, 1493–1502.
- Kang, J. I., and Sowers, L. C. (2008) Examination of hypochlorous acid-induced damage to cytosine residues in a CpG dinucleotide in DNA. *Chem. Res. Toxicol.* 21, 1211–1218.
- Morris, S. M. (1993) The genetic toxicology of 5-fluoropyrimidines and 5-chlorouracil. *Mutat. Res.* 297, 39–51.
- Whiteman, M., Jenner, A., and Halliwell, B. (1997) Hypochlorous acid-induced base modifications in isolated calf thymus DNA. *Chem. Res. Toxicol.* 10, 1240–1246.
- Visser, D. W., Frisch, D. M., and Huang, B. (1960) Synthesis of 5-chlorodeoxyuridine and a comparative study of 5-halodeoxyuridines in *E. coli*. *Biochem. Pharmacol.* 5, 157–164.
- Jaunin, F., Visser, A. E., Cmarko, D., Aten, J. A., and Fakan, S. (1998) A new immunocytochemical technique for ultrastructural analysis of DNA replication in proliferating cells after application of two halogenated deoxyuridine. *J. Histochem. Cytochem.* 46, 1203–1209.
- Svetlova, M., Solovjeva, L., Blasius, M., Shevelev, I., Hubscher, U., Hanawalt, P., and Tomilin, N. (2005) Differential incorporation of halogenated deoxyuridines during UV-induced DNA repair synthesis in human cells. *DNA Repair* 4, 359–366.
- Yamada, K., Semba, R., Ding, X., Ma, N., and Nagahama, M. (2005) Discrimination of cell nuclei in early S-phase, mid-to-late S-phase, and G2/M-phase by sequential administration of 5-bromo-2'-deoxyuridine and 5-chloro-2'-deoxyuridine. *J. Histochem. Cytochem.* 53, 1365–1370.
- Vecchio, L., Solimando, L., Biggiogera, M., and Fakan, S. (2008) Use of halogenated precursors for simultaneous DNA and RNA detection by means of immunoelectron and immunofluorescence microscopy. *J. Histochem. Cytochem.* 56, 45–55.
- Heartlein, M. W., O'Neill, J. P., Pal, B. C., and Preston, R. J. (1982) The induction of specific-locus mutations and sister-chromatid exchanges by 5-bromo and 5-chloro-deoxyuridine. *Mutat. Res.* 92, 411–416.
- DuFrain, R. J. (1984) Probing sister chromatid exchange formation with halogenated pyrimidines. *Basic Life Sci.* 29, 41–58.
- Zwanenburg, T. S., Hansson, K., Darroudi, F., van Zeeland, A. A., and Natarajan, A. T. (1985) Effects of 3-aminobenzamide on Chinese hamster cells treated with thymidine analogues and DNA-damaging agents. Chromosomal aberrations, mutations and cell-cycle progression. *Mutat. Res.* 151, 251–262.
- Brandon, M. L., Mi, L.-J., Chung, W., Teebor, G., and Boorstein, R. J. (2000) 5-Chloro-2'-deoxyuridine cytotoxicity results from base excision repair of uracil subsequent to thymidylate synthase inhibition. *Mutat. Res.* 459, 161–169.
- Michishita, E., Kurahashi, T., Suzuki, T., Fukuda, M., Fujii, M., Hirano, H., and Ayusawa, D. (2002) Changes in nuclear matrix proteins during senescence-like phenomenon induced by 5-chlorodeoxyuridine in HeLa cells. *Exp. Gerontol.* 37, 885–890.
- Polak, M. B., Valamanesh, F., Felt, O., Torriglia, A., Jeanny, J. C., Bourges, J. L., Rat, P., Thomas-Doyle, A., BenEzra, D., Gurny, R., and Behar-Cohen, F. (2008) Controlled delivery of 5-chlorouracil using poly(ortho esters) in filtering surgery for glaucoma. *Invest. Ophthalmol. Vis. Sci.* 49, 2993–3003.
- Kumar, R., Wiebe, L. I., and Knaus, E. E. (1994) A mild and efficient methodology for the synthesis of 5-halogeno uracil nucleosides that occur via a 5-halogeno-6-azido-5,6-dihydro intermediate. *Can. J. Chem.* 72, 2005–2010.
- Van Aerschot, A., Everaert, D., Balzarini, J., Augustyns, K., Jie, L., Janssen, G., Peeters, O., Blaton, N., De Ranter, C., and De Clercq, E.; et al. (1990) Synthesis and anti-HIV evaluation of 2',3'-dideoxyribo-5-chloropyrimidine analogues: Reduced toxicity of 5-chlorinated 2',3'-dideoxynucleosides. *J. Med. Chem.* 33, 1833–1839.
- Cui, Z., Theruvathu, J. A., Farrel, A., Burdzy, A., and Sowers, L. C. (2008) Characterization of synthetic oligonucleotides containing biologically important modified bases by matrix-assisted laser desorption time-of-flight mass spectrometry. *Anal. Biochem.* 379, 196–207.
- Kang, J. I., Burdzy, A., Liu, P., and Sowers, L. C. (2004) Synthesis and characterization of oligonucleotides containing 5-chlorocytosine. *Chem. Res. Toxicol.* 17, 1236–1244.
- Patel, D. J., Kozlowski, S. A., Marky, L. A., Broka, C., Rice, J. A., Itakura, K., and Breslauer, K. J. (1982) Premelting and melting transitions in the d(CGCGAATTCGCG) self-complementary duplex in solution. *Biochemistry* 21, 428–436.

26. Hare, D. R., Wemmer, D. E., Chou, S. H., Drobny, G., and Reid, B. R. (1983) Assignment of the non-exchangeable proton resonances of d(C-G-C-G-A-A-T-T-C-G-C-G) using two-dimensional nuclear magnetic resonance methods. *J. Mol. Biol.* 171, 319–336.
27. Klevit, R. E., Wemmer, D. E., and Reid, B. R. (1986) ¹H NMR studies on the interaction between distamycin A and a symmetrical DNA dodecamer. *Biochemistry* 25, 3296–3303.
28. Sowers, L. C., Fazakerley, G. V., Kim, H., Dalton, L., and Goodman, M. F. (1986) Variation of nonexchangeable proton resonance chemical shifts as a probe of aberrant base pair formation in DNA. *Biochemistry* 25, 3983–3988.
29. Liu, M. L., Mao, X. A., Ye, C. H., Huang, H., Nicholson, J. K., and Lindon, J. C. (1998) Improved WATERGATE Pulse Sequences for Solvent Suppression in NMR Spectroscopy. *J. Magn. Reson.* 132, 125–129.
30. Liu, P., Theruvathu, J. A., Darwanto, A., Lao, V. V., Pascal, T., Goddard, W. III, and Sowers, L. C. (2008) Mechanisms of base selection by the *Escherichia coli* mispaired uracil glycosylase. *J. Biol. Chem.* 283, 8829–8836.
31. Breslauer, K. J., Frank, R., Blocker, H., and Marky, L. A. (1986) Predicting DNA duplex stability from base sequence. *Proc. Natl. Acad. Sci. U.S.A.* 83, 3746–3750.
32. SantaLucia, J. Jr., Allawi, H. T., and Seneviratne, P. A. (1996) Improved nearest-neighbor parameters for predicting DNA duplex stability. *Biochemistry* 35, 3555–3562.
33. Allawi, H. T., and SantaLucia, J. Jr. (1997) Thermodynamics and NMR of internal G·T mismatches in DNA. *Biochemistry* 36, 10581–10594.
34. Weiss, M. A., Patel, D. J., Sauer, R. T., and Karplus, M. (1984) Two-dimensional ¹H NMR study of the λ operator site OLI: A sequential assignment strategy and its application. *Proc. Natl. Acad. Sci. U.S.A.* 81, 130–134.
35. Parker, W. B., and Cheng, Y. C. (1990) Metabolism and mechanism of action of 5-fluorouracil. *Pharmacol. Ther.* 48, 381–395.
36. Wyatt, M. D., and Wilson, D. M. III (2009) Participation of DNA repair in the response to 5-fluorouracil. *Cell. Mol. Life Sci.* 66, 788–799.
37. Liu, P., Burdzy, A., and Sowers, L. C. (2002) Substrate recognition by a family of uracil-DNA glycosylases: UNG, MUG and TDG. *Chem. Res. Toxicol.* 15, 1001–1009.
38. Bennett, M. T., Rodgers, M. T., Hebert, A. S., Ruslander, L. E., Eisele, L., and Drohat, A. C. (2006) Specificity of human thymine DNA glycosylase depends on N-glycosidic bond stability. *J. Am. Chem. Soc.* 128, 12510–12519.
39. Miki, K., Shimizu, M., Fujii, M., Hossain, M. N., and Ayusawa, D. (2008) 5-Bromouracil disrupts nucleosome positioning by inducing A-form-like DNA conformation in yeast cells. *Biochem. Biophys. Res. Commun.* 368, 662–669.
40. Yu, H., Eritja, R. E., Bloom, L. B., and Goodman, M. F. (1993) Ionization of bromouracil and fluorouracil stimulates base mispairing frequencies with guanine. *J. Biol. Chem.* 268, 15935–15943.
41. Dunn, D. B., and Smith, J. D. (1957) Effects of 5-halogenated uracils on the growth of *Escherichia coli* and their incorporation into deoxyribonucleic acids. *Biochem. J.* 67, 494–506.
42. Stetson, P. L., Normolle, D. P., Knol, J. A., Johnson, N. J., Yang, Z. M., Sakmar, E., Prieskorn, D., Terrio, P., Knutsen, C. A., and Ensminger, W. D. (1991) Biochemical modulation of 5-bromo-2'-deoxyuridine and 5-iodo-2'-deoxyuridine incorporation into DNA in VX2 tumor-bearing rabbits. *J. Natl. Cancer Inst.* 83, 1659–1667.
43. Yang, Z., and Rodgers, M. T. (2004) Influence of halogenation on the properties of uracil and its noncovalent interactions with alkali metal ions. Threshold collision-induced dissociation and theoretical studies. *J. Am. Chem. Soc.* 126, 16217–16226.
44. Sowers, L. C., Eritja, R., Kaplan, B. E., Goodman, M. F., and Fazakerley, G. V. (1987) Structural and dynamic properties of a fluorouracil-adenine base pair in DNA studied by proton NMR. *J. Biol. Chem.* 262, 15436–15442.
45. Kremer, A. B., Mikita, T., and Beardsley, G. P. (1987) Chemical consequences of the incorporation of 5-fluorouracil into DNA as studied by NMR. *Biochemistry* 26, 391–397.
46. Fazakerley, G. V., Sowers, L. C., Eritja, R. E., Kaplan, B. E., and Goodman, M. F. (1987) Structural and dynamic properties of a bromouracil-adenine base pair in DNA studied by proton NMR. *J. Biomol. Struct. Dyn.* 5, 639–650.
47. Várnai, P., Canalia, M., and Leroy, J. L. (2004) Opening mechanism of G·T/U pairs in DNA and RNA duplexes: A combined study of imino proton exchange and molecular dynamics simulation. *J. Am. Chem. Soc.* 126, 14659–14667.
48. Guéron, M., and Leroy, J. L. (1995) Studies of base pair kinetics by NMR measurement of proton exchange. *Methods Enzymol.* 261, 383–413.
49. Sternglanz, H., and Bugg, C. E. (1975) Relationship between the mutagenic and base-stacking properties of halogenated uracil derivatives. The crystal structure of 5-chloro- and 5-bromouracil. *Biochim. Biophys. Acta* 378, 1–11.
50. Shulman, R. G. (1969) The double minimum of the adenine-thymine hydrogen bond. *Ann. N.Y. Acad. Sci.* 158, 96–99.
51. Sowers, L. C., Shaw, B. R., Veigl, M. L., and Sedwick, W. D. (1987) DNA base modification: Ionized base pairs and mutagenesis. *Mutat. Res.* 177, 201–218.
52. Zhang, J. D., Chen, Z., and Schaefer, H. F. (2008) Electron attachment to the hydrogenated Watson-Crick guanine cytosine base pair (GC+H): Conventional and proton-transferred structures. *J. Phys. Chem. A* 112, 6217–6226.
53. Noguera, M., Bertran, J., and Sodupe, M. (2008) Cu^{+2/+} cation coordination to adenine-thymine base pair. Effects on intermolecular proton-transfer processes. *J. Phys. Chem. B* 112, 4817–4825.
54. Boulard, Y., Cognet, J. A., Gabarro-Arpa, J., LeBret, M., Sowers, L. C., and Fazakerley, G. V. (1992) The pH dependent configurations of the C·A mispair in DNA. *Nucleic Acids Res.* 20, 1933–1941.
55. Moody, E. M., Brown, T. S., and Bevilacqua, P. C. (2004) Simple method for determining nucleobase pK_a values by indirect labeling and demonstration of a pK_a of neutrality in dsDNA. *J. Am. Chem. Soc.* 126, 10200–10201.
56. Tang, C. L., Alexov, E., Pyle, A. M., and Honig, B. (2007) Calculation of pK_as in RNA: On the structural origins and functional roles of protonated nucleotides. *J. Mol. Biol.* 366, 1475–1496.
57. Ivarie, R. (1987) Thymine methyls and DNA-protein interactions. *Nucleic Acids Res.* 15, 9975–9983.
58. Brennan, C. A., Van Cleve, M. D., and Gumpert, R. I. (1986) The effects of base analogue substitutions on the cleavage by the EcoRI restriction endonuclease of octadeoxyribonucleotides containing modified EcoRI recognition sequences. *J. Biol. Chem.* 261, 7270–7278.
59. Petruska, J., and Horn, D. (1983) Sequence-specific responses of restriction endonucleases to bromodeoxyuridine substitution in mammalian DNA. *Nucleic Acids Res.* 11, 2495–2510.
60. Jansco, A., Botfield, M. C., Sowers, L. C., and Weiss, M. A. (1994) An altered-specificity mutation in a human POU domain demonstrates functional analogy between the POU-specific subdomain and phage λ repressor. *Proc. Natl. Acad. Sci. U.S.A.* 91, 3887–3891.
61. Valinluck, V., Wu, W., Liu, P., Neidigh, J. W., and Sowers, L. C. (2006) Impact of cytosine 5-halogens on the interaction of DNA with restriction endonucleases and methyltransferase. *Chem. Res. Toxicol.* 19, 556–562.
62. Voth, A. R., Hays, F. A., and Ho, P. S. (2007) Directing macromolecular conformation through halogen bonds. *Proc. Natl. Acad. Sci. U.S.A.* 104, 6188–6193.